

Blood Vessel Segmentation and Classification of Diabetic Retinopathy Images using Gradient Operator and Statistical Analysis

Praveen Kumar Reddy Yelampalli, Jagadish Nayak, and Vilas H Gaidhane

Abstract—Retinal blood vessel detection in fundus images is a challenging task. Widely spread blood vessels in diabetic retinopathy effected fundus images can not be accurately segmented using conventional gradient-based edge detection techniques. Accurate detection of blood vessels can give better classification for decisive diagnosis at different stages of diabetic retinopathy. The proposed blood vessel segmentation technique is a combination of gradient and morphological operators. The fundus images are preprocessed using a local-phase-based enhancement technique to highlight the blood vessels from the background image. Further, detected edges are made connected using an averaging filter. Area occupied by the blood vessels provides a biomarker to classify fundus images into normal, prolific diabetic retinopathy (PDR), and non-prolific diabetic retinopathy (NPDR). The classification is achieved using ANOVA test. The ANOVA test classified with the 91% accuracy for normal, 92.7% for PDR, and 87.8% for NPDR images, respectively. These results are compared with conventional Canny and Prewitt edge detection techniques and the proposed method outperforms both.

Index Terms—diabetic retinopathy, edge detection, gradient operator, morphological operations, ANOVA test, classification.

I. INTRODUCTION

DIABETIC retinopathy (DR) commonly appears in diabetic patients which causes blindness due to damaged retina. The retinal structure of DR affected eyes can be seen using fundus imaging technique. Fundus images are usually acquired by a fundus camera focusing through the eye. Fundus images show the internal eye surface consisting of blood vessels, fovea, macula, retina, and optic disc. A healthy retina contains only blood vessels that carrying blood and nutrients required for an eye. These blood vessels are fragile in nature and rupture due to excess blood pressure in diabetic patients. The progress of diabetic retinopathy due to excess pressure can be detected by the growth of extraneous small blood vessels from the surface of the retina. This growth in blood vessels can be used as a bio-marker for classifying different stages of diabetic retinopathy such as PDR and NPDR against the normal retina [1].

In the last decade, many researchers have developed efficient vessel segmentation schemes and classified the retinal images on the basis of disease severity and type [2]-[9]. Nayak *et al.*, [10] proposed an automated retinopathy classification method based on artificial neural network for

the early recognition of DR. This method employs morphological operators to separate blood vessels and exudates. In another approach, fuzzy c means (FCM) and genetic algorithms detected exudates with 96% accuracy [11]. Akram *et al.* [12] presented a multilayered thresholding technique to segment the blood vessels in retinopathy images. Wavelet [13], ridgelets [14] and curvelet [15] transforms are also used with the fundus images for the analysis of retinal structure. A fuzzy logic approach attained a sensitivity of 99.9% for the hard exudate detection in DR images [16].

In 2012, Nguyen *et al.* [17] developed a retinal vascular feature analysis using a multi-scale line detector. Roychowdhury *et al.* [18] developed a DREAM (Diabetic retinopathy analysis using machine learning) project by combining the Gaussian mixer model with the k-nearest neighbourhood algorithm and classified using singular vector machine (SVM). Further, Zhao *et al.* [19] used \mathcal{L}^2 Lebesgue integral method to estimate an infinite perimeter regularization. Global thresholding technique is implemented by Mapayi *et al.* [7] for the preprocessing of retinal images. A morphological component analysis (MCA) of vessel detection has attained an accuracy of 0.959 and 0.9523 with STARE and DRIVE datasets, respectively [20]. Premature retinopathy in blood vessels can be studied by tortuosity level on the retina. Masoud *et al.* [21] presented a curvature-based algorithm for vessel grading depends on the tortuosity levels.

Roychowdhury *et al.* [22] estimated the boundary of the optic disc using a Gaussian mixture model. Liskowski and Krawiec [23] used a deep neural network methodology that trained on a huge samples of DRIVE, STARE and CHEST datasets. However, this method requires a substantial amount of samples (upto 400,000). In a recent work, Seoud *et al.* [24] developed a telemedicine system using the red-lesions for computer-aided screening of retinopathy images. Later, a direct method has been proposed through training the classifier for DR referral [25]. The omission of lesions reduced efforts to detect the lesions, however, it requires large pool of data to train the classifier.

All the existing methods such as wavelets, morphological gradients, neural networks, and other computational intelligent procedures have come across a long way in the effective and accurate detection of DR at the earliest possible stages. However, these techniques are computationally complex and required considerably large training to the classifiers. With the motive of the previous works, in this paper we presented a new and simple fundus image classification technique using ANOVA statistical method. Optical images suffer from improper contrast due to non-uniform lighting condition during acquisition. So as to obtain good contrast image, preprocess-

Manuscript received July 07, 2017; revised July 12, 2017.

P. K. R. Yelampalli, J. Nayak, and V. H. Gaidhane are with the Department of Electrical and Electronics Engineering, BITS Pilani, Dubai Campus, Dubai, 345055 UAE e-mail: praviin.reddy@gmail.com, jagadishnayak@dubai.bits-pilani.ac.in, vhgaidhane@dubai.bits-pilani.ac.in.

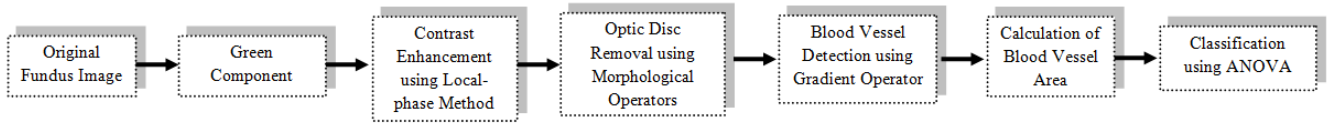


Fig. 1. Framework for DR image vessel detection and classification

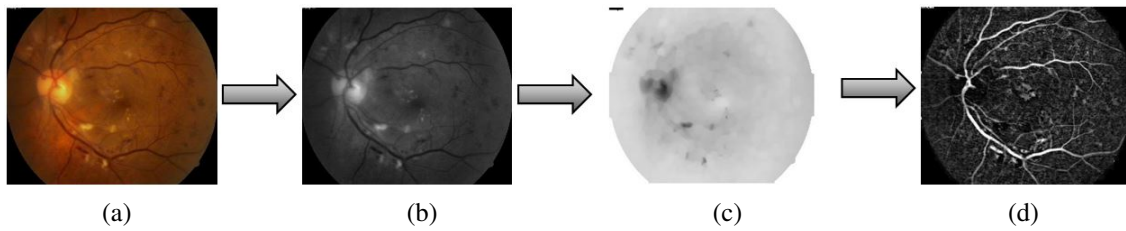


Fig. 2. Removal of optic disc (a) Original image (b) Green component (c) Background obtained using morphological transformation[10] (d) Image with optic disc removed

ing is applied on the acquired fundus images. Later, optic disc is removed using morphological transformation [10] to enable clear blood vessels and exudates visibility in the acquired image. First, the fundus images are contrast enhanced using a local-phase-based quadrature filtering method. The proposed method introduces new method of edge detection to segment blood vessels from all other backgrounds in the fundus image. Further, the density of blood vessels is computed based on the area measure. The total count of pixels which constitute blood vessels is used as a parameter for classification.

The remaining paper is organised as, processes involved in the blood vessel segmentation and classification are explained in Section II. Detailed discuss of experimental results is presented in Section III. Section IV concludes the paper with the further possible extension to the present work.

II. METHODS AND APPROACHES

A. Proposed edge detection method

Fig1 shows the block diagrammatic approach of fundus image blood vessel detection. The green component of RGB fundus image shows prominent blood vessels compared to RED and BLUE components. Hence, we used the GREEN component of the fundus image in our work. At the first stage, for improving the visibility of the regions contrast enhancement [13] is performed using local-phase method [26]. Local-phase method uses quadrature filter to combine both line and edge detectors, and gives better enhancement compared to wavelets, histogram equalization, and other filtering approaches. This strengthen the vessel structures at multiple scales. Fourier domain representation of quadrature filter is

$$F_k(\mathbf{u}) = 0, \quad \mathbf{u} \cdot \mathbf{n}_k \leq 0 \quad (1)$$

where \mathbf{u} and $\mathbf{u} \cdot \mathbf{n}_k$ are frequency and filter direction respectively.

In the present work, the optic disc (OD) is removed by applying a morphological transform [10]. Firstly, the background of the image is evaluated using the transform and it is subtracted from the original image. Fig. 2 shows the step-by-step removal of OD. The transformation function can be defined as

$$I_{transform} = I - (I \circ S) \quad (2)$$

where S is the structuring element of radius $R = 3$ and type 'disc' as shown in Fig. 3.

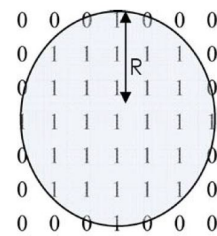


Fig. 3. Disc structuring element with radius $R = 3$

A gradient operator (∇) depicts the slope of a function in a particular direction. In a simplified form ∇ of a function $f(x)$ can be expressed as

$$\nabla f(\mathbf{x}) \cdot \mathbf{v} = D_v f(\mathbf{x}) \quad (3)$$

The first-order gradient vectors $g_x(m, n)$ and $g_y(m, n)$ for an image $I(m, n)$ in horizontal (k_x) and vertical (k_y) directions are [27]

$$\begin{aligned} g_x(m, n) &= I(m, n) * k_x \\ g_y(m, n) &= I(m, n) * k_y \end{aligned} \quad (4)$$

The calculated gradient vectors $g_x(m, n)$ and $g_y(m, n)$ in equation 4 are normalized with the magnitude to obtain the unit gradient vectors $u_x(m, n)$ and $u_y(m, n)$

$$\begin{aligned} u_x(m, n) &= g_x(m, n) / \sqrt{g_x^2(m, n) + g_y^2(m, n)} \\ u_y(m, n) &= g_y(m, n) / \sqrt{g_x^2(m, n) + g_y^2(m, n)} \end{aligned} \quad (5)$$

This method considers only the magnitude component for blood vessel extraction. Fig. 4 shows the blood vessel extraction using the proposed method. The images from top to bottom are the normal, PDR, and NPDR in the order of appearance. Resulting images contains some non-connected components which are removed by applying an average filtering with adaptive thresholding. Finally, area of the blood vessels is evaluated as the non-zero pixel count in the resulting image. Next section presents the results and the classification using statistical method.

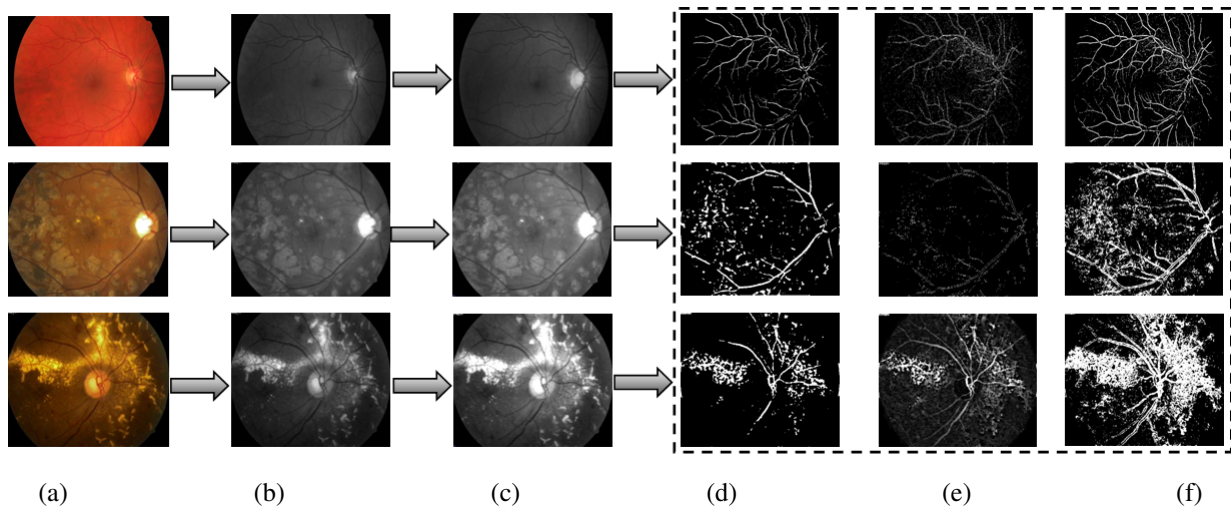


Fig. 4. Row-wise: Normal, PDR, and NPDR images. (a) Original fundus image (b) Green component of the original (c) Enhanced green component using local-phase [26] (d) Blood vessels detected using Canny edge detection (e) Blood vessels detected using Prewitt method (f) Blood vessels detected using the proposed method

B. ANOVA Statistical test

The ANOVA (Analysis of variance) statistical test gives the statistical dependency of three or more unrelated groups. The statistical difference between the means and the variance are estimated by plotting the boxplots. A boxplot is a graphical representation of numerical data using quartiles. As depicted in Fig. 5, a boxplot consists of maximum and minimum values of the dataset, median of the values in each dataset, quartiles (first and third), inner fence, outer fence, and whiskers. First quartile represents the variance from the median to the minimum value whereas, third quartile gives the variance from median to the maximum value in the dataset. Whiskers are the vertically extended lines from the quartiles indicate the variability outside the two quartiles. The inner fence shows the likely presence of values beyond one and half times of the variance and these are called suspected outliers. Similarly, the outer fence is the boundary the values beyond which are considered to be outliers [28].

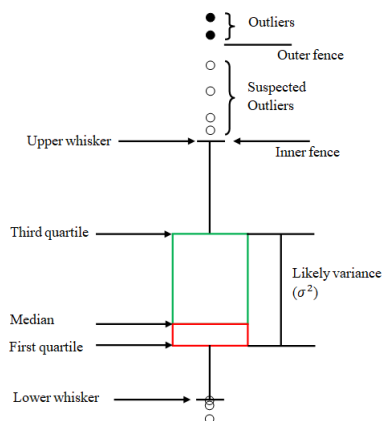


Fig. 5. Boxplot description.

III. RESULTS AND DISCUSSIONS

Retinal images of 140 subjects aged between 25-57 years have been collected at Department of Ophthalmology, Kasturba Medical College, Manipl, India. A TRC-NW200

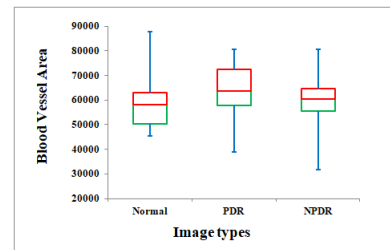


Fig. 6. Boxplots representing the classification of normal, PDR, and NPDR based on blood vessel area in each image category using Canny.

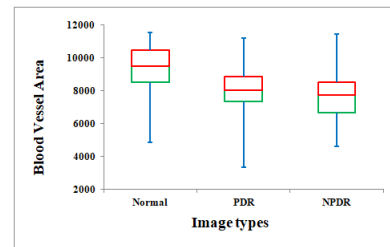


Fig. 7. Boxplots representing the classification of normal, PDR, and NPDR based on blood vessel area in each image category using Prewitt.

model TOPCON mydriatic retinal camera has used for image acquisition. All the images have the resolution of 560×720 . In this experimentation images of normal, prolific DR, and non-prolific DR are considered for the classification. Blood vessels are extracted using the methods discussed in Section II. Further, blood vessel area (A) of each image is determined using equation (6)

$$A = \sum_i \sum_j \Omega_{i,j} \quad \forall \quad \Omega_{i,j} \neq 0 \quad (6)$$

The area obtained for all the images are separated and plotted using the box plots. Box plot represents maximum value, minimum value, mean, and variances of a given sequence of N elements. The p -value calculated for this method is $p < 1 \times 10^{-4}$. Overlapping regions in the box plot depict that the values in the two sequences have statistical dependency. Otherwise, they are independent and define the classification of the two sets considered.

TABLE I
MEAN AND VARIANCES OF BLOOD VESSEL AREAS CALCULATED FOR EACH CLASS OF RETINAL IMAGES USING CANNY, PREWITT, AND THE PROPOSED METHOD. THE p -VALUE IS $< 1 \times 10^{-4}$

Method	Canny			Prewitt			Proposed		
	Normal	PDR	NPDR	Normal	PDR	NPDR	Normal	PDR	NPDR
Mean	58145	63670	60374	9518	8025.5	4609	349274	359521	363414
Variance	± 8053.7	± 9492.1	± 9890.8	± 1596.2	± 1332.6	± 1282.7	± 4809.0	± 3840.8	± 4587.2
Accuracy	73.4%	77.7%	68.5%	74.2%	56.9%	61.1%	91%	92.7%	87.8%

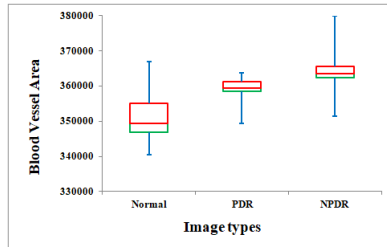


Fig. 8. Boxplots representing the classification of normal, PDR, and NPDR based on blood vessel area in each image category using the Proposed method.

The boxplots for blood vessel area calculated using Canny edge detection are shown in Fig. 6. This shows significant overlapping between any two classes and hence they are statistically dependent. Hence the Canny method results in poor accuracy of 73.4%, 77.7%, and 68.5% for normal, PDR, and NPDR retinopathy images, respectively. The accuracy is not acceptable in the clinical diagnosis of retinopathy. On the other hand, vessel area calculated using a Prewitt-based method is achieved 74.2%, 56.9%, and 61.1% accuracy of classification between normal, PDR, and NPDR images. This is due to the fact that the Prewitt edges are unable to specify blood vessels precisely in healthy and retinopathy images. The ANOVA statistical plots for Prewitt method are shown in Fig. 7.

However, From Fig. 8 it is evident that the considered images of three classes are statistically independent with respect to the blood vessel area. Table. I shows the average area obtained for normal, PDR, and NPDR images. Moreover, the variance gives the maximum and minimum vessel areas for each class of images. Accuracy of the present method is evaluated based on the number of images having the blood vessel area beyond the mean and variance values calculated for each image category. The accuracy of the proposed classification method is 91% for normal, 92.7% for PDR, and 87.8% for NPDR images. The superiority of the proposed method is its efficiency in the classification of retinal fundus images when compared to the conventional Canny and Prewitt edge detectors.

IV. CONCLUSION AND FUTURE SCOPE

The proposed methodology for blood vessel detection classifies retinal fundus images of diabetic patients. The combination of gradient operator and morphological operations highlights the blood vessels in the retinal fundus image more clearly than conventional edge detection operations. The area contributed by the detected blood vessels is used as feature for classification. The ANOVA test statistically classified fundus images as normal, PDR, and NPDR. The classification accuracy is high in the proposed method due

to the clear visibility of blood vessels as a biomarker which distinguishes the fundus image into three classes. Better accuracy can be achieved by taking more features other than blood vessel areas and efficient noise removal techniques. In recent days, binary patterns are also emerging as reliable edge detectors with smaller feature size and exceptional local texture analysis.

REFERENCES

- [1] C. P. Wilkinson, F. L. Ferris, R. E. Klein, P. P. Lee, C. D. Agardh, M. Davis, D. Dills, A. Kampik, R. Parajasegaram, and J. T. Verdager, "Proposed international clinical diabetic retinopathy and diabetic macular edema disease severity scales," *Ophthalmology*, vol. 110, no. 9, pp. 1677–1682, Sep. 2003.
- [2] M. M. Fraz, P. Remagnino, A. Hoppe, B. Uyyanonvara, A. R. Rudnicka, C. G. Owen, and S. A. Barman, "Blood vessel segmentation methodologies in retinal images -A Survey," *Comput. Meth. Prog. Bio.*, vol. 108, pp. 407–433, Mar. 2012.
- [3] J. Nayak, P. S. Bhat, and U. R. Acharya, "Automatic identification of diabetic maculopathy stage using fundus images," *J. Med. Eng. Technol.*, vol. 33, no. 2, pp. 119–129, Feb. 2009.
- [4] K. Ram, G. D. Joshi, and J. Sivaswamy, "A successive clutter-rejection-based approach for early detection of diabetic retinopathy," *IEEE Trans. Biomed. Eng.*, vol. 58, no. 3, pp. 664–673, Mar. 2011.
- [5] M. M. Fraz, P. Remagnino, A. Hoppe, B. Uyyanonvara, A. R. Rudnicka, C. G. Owen, and S. A. Barman, "An ensemble classification-based approach applied to retinal blood vessel segmentation," *IEEE Trans. Biomed. Eng.*, vol. 59, no. 9, pp. 2538–2548, Sep. 2012.
- [6] S. W. Franklin and S. E. Rajan, "Diagnosis of diabetic retinopathy by employing image processing technique to detect exudates in retinal images," *IET Image Process.*, vol. 8, no. 10, pp. 601–609, 2014.
- [7] T. Mapayi, S. Viriri, and J-R. Tapamo, "Comparative study of retinal vessel segmentation based on global thresholding techniques," *Comput. Math. Method. M.*, vol. 2015, pp. 1–15, Nov. 2014.
- [8] D. Wu, M. Zhang, J-C. Liu, and W. Bauman, "On the adaptive detection of blood vessels in retinal images," *IEEE Trans. Biomed. Eng.*, vol. 53, no. 2, pp. 341–343, Feb. 2006.
- [9] A. M. Mendinca and A. Campilho, "Segmentation of retinal blood vessels by combining the detection of centerlines and morphological reconstruction," *IEEE Trans. Med. Imag.*, vol. 25, no. 9, pp. 1200–1213, Sep. 2006.
- [10] J. Nayak, P. S. Bhat, U. R. Acharya, C. M. Lim, and M. Kagathi, "Automated identification of diabetic retinopathy stages using digital fundus images," *J. Med. Syst.*, vol. 32, pp. 107–115, 2008.
- [11] A. Osareh, B. Shadgar, and R. Markham, "A computational-intelligence-based approach for detection of exudates in diabetic retinopathy images," *IEEE Trans. Inf. Technol. Biomed.*, vol. 13, no. 4, pp. 535–545, Jul. 2009.
- [12] M. U. Akram and S. A. Khan, "Multilayered thresholding-based blood vessel segmentation for screening of diabetic retinopathy," *Eng. Comput.*, vol. 29, pp. 165–173, 2013.
- [13] P. Bankhead, C. N. Scholfield, J. G. McGeown, and T. M. Curtis, "Fast retinal vessel selection and measurement using wavelets and edge location refinement," *PLOS One*, vol. 7, no. 3, pp. 1–12, Mar. 2012.
- [14] J. Staal, M. D. Abramoff, M. Niemeijer, M. A. Viergever, and B. v. Ginneken, "Ridge-based vessel segmentation in color images of the retina," *IEEE Trans. Med. Imag.*, vol. 23, no. 4, pp. 501–509, Apr. 2004.
- [15] M. S. Miri and A. Mahloojifar, "Retinal image analysis using curvelet transform and multistructure elements morphology by reconstruction," *IEEE Trans. Biomed. Eng.*, vol. 58, no. 5, pp. 1183–1192, May 2011.
- [16] N. G. Ranamuka and R. G. N. Meegama, "Detection of hard exudates from diabetic retinopathy images using fuzzy logic," *IET Image Process.*, vol. 7, no. 2, pp. 121–130, 2013.

- [17] U. T. V. Nguyen, A. Bhuiyan, L. A. F. Park, and K. Ramamohanarao, "An effective retinal blood vessel segmentation method using multi-scale line detection," *Pattern Recogn.*, vol. 46, pp. 703–715, 2013.
- [18] S. Roychowdhury, D. D. Koozekanani, and K. K. Parhi, "DREAM: Diabetic retinopathy analysis using machine learning," *IEEE J. Biomed. Health Inform.*, vol. 18, no. 5, pp. 1717–1728, Sep. 2014.
- [19] Y. Zhao, L. Rada, K. Chen, S. P. Harding, and Y. Zheng, "Automated vessel segmentation using infinite perimeter active contour model with hybrid region information with application to retinal images," *IEEE Trans. Med. Imag.*, vol. 34, no.9, pp. 1797–1807, Sep. 2015.
- [20] E. Imani, M. Javidi, and H-R. Pourreza, "Improvement of retinal blood vessel detection using morphological component analysis," *Comput. Meth. Prog. Bio.*, vol. 118, pp. 263–279, 2015.
- [21] A-S. Masoud, H. R. Pourreza, and T. Banaee, "A novel curvature-based algorithm for automatic grading of retinal blood vessel tortuosity," *IEEE J. Biomed. Health Inform.*, vol. 20, no. 2, pp. 586–595, Mar. 2016.
- [22] S. Roychowdhury, D. D. Koozekanani, S. N. Kuchinka, and K. K. Parhi, "Optic disc boundary and vessel origin segmentation of fundus images," *IEEE J. Biomed. Health Inform.*, vol. 20, no. 6, pp. 1562–1574, Nov. 2016.
- [23] P. Liskowski and K. Krawiec, "Segmenting retinal blood vessels with deep neural networks," *IEEE Trans. Med. Imag.*, vol. 35, no. 11, pp. 2369–2380, Nov. 2016.
- [24] L. Seoud, T. Hurtut, J. Chelbi, F. Cheriet, and, J. M. P. Langlois, "Red lesion detection using dynamic shape features for diabetic retinopathy screening," *IEEE Trans. Med. Imag.*, vol. 35, no. 4, pp. 1116–1126, Apr. 2016.
- [25] R. Pires, S. Avila, H. F. Jelinek, J. Wainer, E. Valle, and A. Rocha, "Beyond lesion-based diabetic retinopathy: a direct approach for retinal," *IEEE J. Biomed. Health Inform.*, vol. 21, no. 1, pp. 193–200, Jan. 2017.
- [26] G. L  th  n, J. Jonasson, M. Borga, "Blood vessel segmentation using multi-scale quadrature filtering," *Pattern Recogn. Lett.*, vol. 31, no. 8, pp. 762–767, Jun. 2010.
- [27] D. Onkaew, R. Turior, B. Uyyanonvara, and T. Kondo, "Automatic extraction of retinal vessels based on gradient orientation analysis," in *Int. Joint Conf. Comput. Sci. Softw. Eng.*, 2011, pp. 102–105.
- [28] T. L. Weissgerber, N. M. Milic, S. J. Winham, and V. D. Garovic, "Beyond bar and line graphs: Time for a new data presentation paradigm," *PLoS Biol.*, vol. 13, no. 4, Apr. 2015.